Title

Dynamic UltraFast 2D EXchange SpectroscopY (UF-EXSY) of hyperpolarized substrates

Authors

Swisher, Christine Leon

Koelsch, Bertram

Sukumar, Subramianam

et al.

Publication Date

2015-08-01

DOI

10.1016/j.jmr.2015.05.011

Peer reviewed

HHS Public Access

Author manuscript

J Magn Reson. Author manuscript; available in PMC 2016 August 01.

Published in final edited form as:

J Magn Reson. 2015 August ; 257: 102–109. doi:10.1016/j.jmr.2015.05.011.

Dynamic UltraFast 2D EXchange SpectroscopY (UF-EXSY) of hyperpolarized substrates

Christine Leon Swisher[a,b], **Bertram Koelsch**[a,b], **Subramianam Sukumar**[a], **Renuka Sriram**[a], **Romelyn Delos Santos**[a], **Zhen Jane Wang**[a], **John Kurhanewicz**[a,b], **Daniel Vigneron**[a,b,*], and **Peder Larson**[a,b,*]

[a]Department of Radiology and Biomedical Imaging, University of California, San Francisco, United States

[b]UC Berkeley-UCSF Graduate Program in Bioengineering, University of California, San Francisco and University of California, Berkeley, United States

Abstract

In this work, we present a new ultrafast method for acquiring dynamic 2D EXchange SpectroscopY (EXSY) within a single acquisition. This technique reconstructs two-dimensional EXSY spectra from one-dimensional spectra based on the phase accrual during echo times. The Ultrafast-EXSY acquisition overcomes long acquisition times typically needed to acquire 2D NMR data by utilizing sparsity and phase dependence to dramatically undersample in the indirect time dimension. This allows for the acquisition of the 2D spectrum within a single shot. We have validated this method in simulations and hyperpolarized enzyme assay experiments separating the dehydration of pyruvate and lactate-to-pyruvate conversion. In a renal cell carcinoma cell (RCC) line, bidirectional exchange was observed. This new technique revealed decreased conversion of lactate-to-pyruvate with high expression of monocarboxylate transporter 4 (MCT4), known to correlate with aggressive cancer phenotypes. We also showed feasibility of this technique *in vivo* in a RCC model where bidirectional exchange was observed for pyruvate–lactate, pyruvate–alanine, and pyruvate–hydrate and were resolved in time. Broadly, the technique is well suited to investigate the dynamics of multiple exchange pathways and applicable to hyperpolarized substrates where chemical exchange has shown great promise across a range of disciplines.

Keywords

Hyperpolarized; ^{13}C; EXSY; Stimulated echo; 2D NMR; MCT4; Chemical exchange; Ultrafast

1. Introduction

In the fields of chemistry and biology, multidimensional Nuclear Magnetic Resonance (NMR) acquisitions, which differentiate and correlate the resonances arising from individual sites onto multiple frequency axes, are commonly used to study structure, dynamics, reaction states, proteins, the chemical environment of molecules, or any other sample that

*Corresponding authors at: Byers Hall, Room 102C, 1700 4th St, San Francisco, CA 94158, United States. Dan.Vigneron@ucsf.edu (D. Vigneron), Peder.Larson@ucsf.edu (P. Larson).

contains nuclei possessing spin [1–3]. These experiments are intrinsically longer than their conventional one-dimensional (1D) counterparts. In general, 2D NMR techniques are limited by the inherent low sensitivity, resulting in acquisition times on the order of minutes to hours [1]. In carbon-13 NMR, this is particularly pronounced where less than 1% of carbon atoms possess the NMR detectable ^{13}C isotope. Moreover, SNR suffers from an intrinsically lower gyromagnetic ratio of the ^{13}C isotope.

Not surprisingly, there has been an increased interest in using nuclei in the 'hyperpolarized' state, whose spin population differences depart significantly from the $\approx 10^{-5}$ Boltzmann distribution. Dynamic Nuclear Polarization (DNP) yields over a 10,000-fold increase in SNR [2], which is far greater than what can be achieved by multiscan signal averaging. Hyperpolarization with its dramatic increase in sensitivity provides a unique opportunity to probe previously undetectable phenomena via NMR.

Signal detection of hyperpolarized substrates, however, is challenging due to nonrenewable longitudinal magnetization and short-lived signals. These challenges make conventional 2D NMR acquisition strategies incompatible with hyperpolarized substrates. Specifically, conventional acquisitions schemes for multidimensional NMR require an array of scans that are identical to one another aside from the serial incrementing of evolution delays. Given the non-renewable polarization and the shortened acquisition times due to signal decay by T_1, 2D NMR acquisitions with hyperpolarized substrates requires sequence modifications.

Shapiro and Frydman proposed a method for thermally polarized samples, where the serial indirect domain t_1 encoding of 2D NMR is replaced by a parallelized procedure allowing for different positions within a sample for inequivalent evolution times [4]. Then Frydman and Blazina extended this method to hyperpolarized substrates [1]. We propose a similar method utilizing their parallelized approach as the foundation for this work. The method presented here differs in several aspects: (1) it uses a symmetric slice selective excitation rather than a gradient acting in combination with a frequency-swept excitation for preparation and (2) it uses dephasing and rephasing gradients rather than an oscillating field gradient. The acquisition and reconstruction presented here relies on principles of phase accrual, which expands on our recently described 1D method Metabolic Activity Decomposition with Simulated Echo Acquisition Mode (MAD-STEAM) [5].

The key advancement presented in this work is its application to dynamic 2D EXchange SpectroscopY (EXSY) of hyperpolarized carbon-13 substrates, which we show can be used to detect bidirectional exchange. Exchange is particularly important, where both preclinical cell and animal studies of hyperpolarized substrates [5,9], as well as the first-in-man clinical trial [10], have focused heavily on the exchange of hyperpolarized metabolites as markers of disease.

Magnetic Resonance Spectroscopy of hyperpolarized substrates provides a new tool for investigating tissue metabolism and kinetics *in vivo* [11,12]. Previously experiments using MAD-STEAM showed that in addition to increased conversion of pyruvate-to-lactate in tumors, the less studied conversion of lactate-to-pyruvate was significantly smaller in tumors compared to normal tissue with a transgenic model of prostate cancer [13],

consistent with a decreased LDH-B expression and increased monocarboxylate transporter 4 (MCT4) and LDH-A expression. However, the rate as measured can be corrupted by alanine-to-pyruvate and hydrate-to-pyruvate conversion, warranting a method to separate these signals to reveal the origin of this change.

Investigation of bidirectional flux and exchange has a number of applications to the metabolism field such as reductive carboxylation [14,15], lipogenesis and its regulation of citrate and α-ketoglutarate [15], glutamine addiction [17–20], gluconeogenesis, and the isoenzyme composition of LDH. Detection of these pathways has diagnostic and biomedical research potential. For instance, the directionality of reactions within the citric acid cycle has become an area of increased interest as reductive carboxylation has been shown to support tumor growth [14]. However, the signal from hyperpolarized experiments reports only on the bulk spin-exchange and cannot differentiate concomitant spin-exchange. 2D NMR techniques for hyperpolarized substrates could be further used to probe directionality of metabolic pathways. Moreover, 2D NMR could provide improved specificity to cancer metabolism and shed light on exchange and flux of hyperpolarized substrates.

2. Theory

2.1. Acquisition

Conventional dynamic EXSY acquisition schemes necessitate renewable longitudinal magnetization not available in hyperpolarized substrates. Additionally, conventional EXSY acquisition schemes require many repetitions to obtain the entire indirect spectral dimension (Fig. 1a). The dynamic UF (ultra fast)-EXSY pulse sequence is rapid and does not require renewable longitudinal magnetization making it ideal for hyperpolarized substrates (Fig. 1b). Key features include the symmetric slice selection gradient played with the first 90° RF pulse, gradients blips, which rephase echoes sequentially, and a small flip angle for the final RF pulse, which allows for dynamic acquisition of 2D EXSY spectra. The data can be used to measure build up curves for multiple species that can be fit to an exchange model for extraction of kinetic rates of interconversion (Fig. 1c and d).

Since the method relies on stimulated echoes with gradient encoding, it is sensitive to motion and diffusion. For diffusion, high b-values can accelerate signal decay between TMs, shortening the measured T1 relaxation times (“effective T1” times[13]). In this work, we minimized the effect of diffusion by using short, low amplitude gradients, resulting in *b*-values <10 s/mm^2. Bulk motion would result in overall phase shift, however, a ^{13}C-Urea reference signal can be used to correct for the phase shift (Supplemental Fig. 1). Incoherent motion (e.g. turbulent flow) or non-rigid motion will result in additional unrecoverable signal losses. To prevent these losses in cell experiments, flow through the bioreactor was disabled during the signal acquisition.

This method also assumes spatial homogeneity within the voxel. To limit the effects of this assumption, we limited the number of echoes to the minimum requirement such that the inverse problem is not ill-posed. In the case of HP $^{13}C_1$ pyruvate only 2–3 echoes are required to resolve concomitant exchanging spins. This limits the size of the assumed homogenous region.

2.2. Reconstruction

Conventional EXSY reconstruction methods require many τ repetitions to reconstruct the 2D spectra. However, by choosing the τ repetitions wisely, only a few repetitions can be used to acquire an entire 2D sparse spectra. The UF-EXSY reconstruction, shown in Fig. 2, reconstructs the entire 2D spectra from only a few echoes (Fig. 2) with high spectral resolution in the indirect frequency dimension.

The reconstruction relies on the phase accrual, $\Delta\varphi$, of exchanging spins with a resonance frequency difference, Δf, at each echo time, τ, which has been used to directly observe flux and exchange of a single reaction in real-time [5]. For each frequency, f_i, with a signal greater than the noise threshold in the direct frequency direction the cross peaks are calculated using the following equation:

$$S(f_1,f_2)=\begin{cases}\frac{Imag\{S(f_1,f_2)\}}{\sin(2\pi(f_1-f_2)\tau)}, & f_1\neq f_2\\ Re\{S(f_1,f_2)\}-\sum_i\frac{Imag\{S(f_1,f_2)\}}{\tan(2\pi(f_1-f_2)\tau)}, & f_1=f_2\end{cases} \quad (1)$$

By using the real and imaginary spectra, the 2D spectra can be reconstructed from a single echo utilizing the phase accrual, $\Delta\varphi$, between all other frequencies with a signal greater than the noise threshold. However, multiple echo times need to be used to correct for concomitant exchange pathways at a single resonance such that $\Delta\varphi$ varies between the exchange pathways. Additionally it is required that for at least one echo the phase accrual does not equal zero ($\Delta\varphi\neq 0$). With these criteria fulfilled, the problem is no longer an ill-posed inverse problem. As the number of echoes increases, the accuracy will increase. To ensure accuracy at least one unique echo is required for each concomitant spin exchange. For instance in the renal cell carcinoma model, UOK262, there are three possible concomitant spin exchanges at pyruvate's resonance, namely lactate-to-pyruvate, hydrate-to-pyruvate, and alanine-to-pyruvate. Because alanine SNR is below the noise threshold, we only need two echoes to accurately reconstruct the data (Fig. 2).

There will be a small loss in SNR at each repetition due to parsing of the signal. Fortunately, much of the original SNR can be recovered. Where the SNR of a cross peak is a function of τ_i and is defined by

$$SNR(\Delta f)=\frac{S}{n\sigma}\left(\frac{1}{\sin(\Delta\varphi(\tau_1))}+\frac{1}{\sin(\Delta\varphi(\tau_2))}+\cdots\frac{1}{\sin(\Delta\varphi(\tau_n))}\right) \quad (2)$$

where n is the number of echoes. As stated previously, to detect a cross peak it is necessary that for at least one echo the phase must be not be equal to 0 and π ($\pm k$ rotations) with sufficient SNR.

More generally, the entire spectra can be described by the following equations:

$$cross\ peaks: X=A^{(-1)}a \quad (3)$$

$$diagonal{:}Y=b-\sum_{f}XB \quad (4)$$

where

$$A=\begin{bmatrix} \sin(\varphi_{1,\tau 1}) & \sin(\varphi_{1,\tau 2}) & \cdots \\ \sin(\varphi_{2,\tau 1}) & \sin(\varphi_{2,\tau 2}) & \cdots \\ \vdots & \vdots & \ddots \end{bmatrix} \quad a=\begin{bmatrix} Im\{S(\tau_1)\} \\ Im\{S(\tau_2)\} \\ \vdots \end{bmatrix}$$
$$B=\begin{bmatrix} \cos(\varphi_{1,\tau 1}) & \cos(\varphi_{1,\tau 2}) & \cdots \\ \cos(\varphi_{2,\tau 1}) & \cos(\varphi_{2,\tau 2}) & \cdots \\ \vdots & \vdots & \ddots \end{bmatrix} \quad b=Re\{S(\tau_1)\}+Re\{S(\tau_1)\}+\cdots \quad (5)$$

Such that the 2D reconstructed spectra can be described by the following equation:

$$\mathbf{2D\ Spectra}=\mathbf{X}+diag(\boldsymbol{Y}) \quad (6)$$

where

$$\mathrm{X}(f_i)=\begin{bmatrix} New\{S(f_i \rightarrow f_0)\} \\ New\{S(f_i \rightarrow f_1)\} \\ \vdots \end{bmatrix} \quad (7)$$

and

$$Y(f_i)=Orig\{S(f_i)\} \quad (8)$$

The reconstruction is summarized in Fig. 2, where selectively sampled FIDs are first reconstructed with 1D Fourier transforms. All frequency locations with an SNR less than the noise (mean + variance) were set below the threshold. The phase accrual for those frequency locations was automatically determined based on their frequency shift and the dephasing time. Finally, a least squares solution was used to obtain the 2D spectra.

In the case of low SNR not observed in this work, noise amplification can be reduced by choosing echo times based on a priori knowledge of cross peak locations. Additionally, noise amplification could be reduced with Tikhonov Regularization. The UF-EXSY reconstruction workflow used in this work is summarized in Supplemental Fig. 1.

3. Methods

3.1. NMR experiments

These studies were conducted on a 14.1T wide-bore microimaging spectrometer equipped with 100 G/cm gradients and a 10 mm broadband probe (Agilent Technologies). The sequence shown in Fig. 1b was acquired with $\Delta\tau$ = 8.575 ms, t_{phase} = 52 μs, G_{phase} = 5 G/cm, t_{crush} = 10 ms, G_{crush} = 15 G/cm, N_{echo} = 3, *TM* = 1–2 s temporal resolution, N_{TM} = 5–20 repetitions, Δ*z* = 3 mm, 20° flip, 64 spectral points, and 4006 Hz bandwidth. Noise was

subtracted to remove cross peak artifacts. T_2 signal loss between echoes was small and considered negligible because of the long T_2s of the hyperpolarized substrates [21]. However, in the case of short T_2s, signal loss between echoes be can corrected in the reconstruction. The number of echo times acquired was always chosen to equal to or greater than the maximum number of concomitant spin exchanges at a single resonance, typically 2–3 for pyruvate. The NMR signal was pre-processed with a 20 Hz Gaussian spectral apodization window on the symmetric echo and zero order spectral phase correction using HP ^{13}C Urea as a reference.

3.2. Polarization of [1-^{13}C] pyruvate and ^{13}C-Urea

[1-^{13}C]-Pyruvate mixed with the trityl radical OX063 (Tris[8-c arboxyl-2,2,6,6tetra[2-(1hydroxyethyl)]-benzo(1,2-d:4,5-d)bis(1,3)dithiole-4-yl]methyl sodium salt, Oxford Instruments, Abingdon UK) was hyperpolarized using conventional DNP methods and a HyperSense DNP polarizer (Oxford Instruments, Abingdon, UK) operating at 3.3T and a temperature of 1.3 K. For validations studies, [1-^{13}C]-Pyruvate was copolarized [22] with ^{13}C-urea mixed with the trityl radical OX063. All samples were dissolved to produce solutions with 80 mM pyruvate and 80 mM urea and a biologically appropriate pH (~7.4) with TRIS/NaOH/EDTA dissolution media. The microwave power was 20mW and the frequency was 94.1 GHz.

3.3. Cell studies

The UOK262 cell line was derived from a metastasis of a highly aggressive hereditary leiomyomatosis RCC (HLRCC) [18]. As described previously by Keshari et al. [8], cells were grown in Dulbeco's Modified Eagle's Medium (DMEM) with 4.5 g/L glucose and then passaged serially. At passages 2–10 and at 60–80% confluency the cells were used for assays and magnetic resonance experiments. This cell lines was chosen because of its high expression of the monocarboxylate transporter 4 (MCT4), which regulates lactate efflux out of the cell as well as for its high lactate dehydrogenase (LDH) activity [8].

3.4. Hyperpolarized ^{13}C magnetic resonance bioreactor experiment

As previously described [7], cells were electrostatically encapsulated into 2.5% w/v alginate microspheres. The microspheres were then loaded into a magnetic resonance–compatible bioreactor and perfused within the bioreactor with DMEM H-21 media at 37 °C maintained 95% air/5% CO_2. Prior to and after spectroscopy experiments, media was perfused with a flow rate of 0.5 mL/min. During acquisition, however, the flow was stopped for the duration of the EXSY acquisition (60 s) to prevent metabolites from flowing-out of the bioreactor. 5 μL of the HP dissolution product was injected over 60 s.

3.5. LDH validation experiments

A 4.5 mL buffered solution (pH ~7.4) of HP pyruvate and HP urea (7.5 μL and 15 μL, respectively, of each formulation described previously [5]) was prepared. 15 mg of NADH and 5 mg of LDH (isoenzyme III, isolated from bovine heart, 646 units/mg protein) in 2 mL phosphate buffer solution were added to 2 mL of the HP dissolution product. The solution

was mixed vigorously and the acquisition was started immediately after. Saturation experiments used a CHESS saturation scheme [5].

3.6. MCT4 inhibition

The inhibitor 4,4-diisothiocyanatostilbene-2,2-disulfonate (DIDS) was chosen based on its preference for MCT4 [23]. UF-EXSY experiments with hyperpolarized $^{13}C_1$-Pyruvate were acquired before and 40 min after the administration of 1 mM DIDS in a UOK262 cell line in a bioreactor.

3.7. In Vivo

To show feasibility a UOK262 cell line was implanted in the renal capsule of Rag2 immunocompromised mouse. 80 mM HP $^{13}C_1$-Pyruvate and ^{13}C-Urea buffered solution (pH ~7.4, 300 μL of the HP dissolution product) was injected over 15 s. Acquisition started at 20 s after the start of injection. 8 mm × 8mm × 8mm voxels were acquired in both the normal and abnormal kidney. The pulse sequence was adapted to be able to select multiple voxels with the addition of slice selection gradients played during the second and third RF pulses (shown in Fig. 5a).

4. Results and discussion

4.1. Validation

The method was validated with a Bloch simulator (SpinBench, Heartvista, Palo Alto, CA) and with hyperpolarized phantom experiments where the hydration of pyruvate and LDH enzymatic activity were observed dynamically (Fig. 3a). To further validate the technique, pyruvate was saturated after allowing hyperpolarized pyruvate to be converted to hyperpolarized lactate via the LDH enzyme and cofactor NADH (Fig. 3a). As expected, only the conversion of lactate-to-pyruvate was observed.

In Fig. 3b, we show that the expected phase shift matches our actual phase shift in a cell study. Here both forward and backward exchange of pyruvate–lactate and pyruvate–hydrate was resolved (Fig. 3c) and acquired dynamically (Supplemental Fig. 3).

4.2. Bidirectional exchange

To investigate the sensitivity of the technique to detect bidirectional exchange, the technique was applied to hyperpolarized pyruvate perfused over renal cell carcinoma (RCC) cell line in a bioreactor to produce 2D EXSY spectra (Fig. 3c). The metastatic RCC cell line (UOK262) was used as a model due to its characteristic elevated expression of MCT4 (Slca16a3), which is known to be indicative of aggressive cancer phenotypes [23–25]. The detection of the activity of a membrane transporter such as MCT4 remains a challenge. We hypothesized that the rate of lactate-to-pyruvate exchange is altered by MCT4 by changing the proximity of lactate to the enzyme as well as altering the intracellular pool size.

4.3. Transport modulates flux

To better isolate the effect of MCT4 on bidirectional exchange, the MCT4 inhibitor, DIDS, was administered in the UOK262 cell line. There was no statistical difference in the flux of

HP pyruvate-to-lactate before and after the addition of the selective MCT4 inhibitor (Fig. 4a). However, the inhibitor resulted in a statistically significant increase (95% Confidence Interval, paired students *t*-test) in the conversion of lactate-to-pyruvate conversion (Fig. 4a). The increased observance of lactate-to-pyruvate flux in the DIDS treated UOK262 cells compared to untreated cells, suggests that efflux of lactate is the major deterrent to lactate-to-pyruvate flux in the UOK262 cell line. To explain this result, we hypothesize that pool-size effects modulate flux (Fig. 4b). HP lactate is more likely to be extracellular when MCT4 is highly expressed and less likely to interact with intracellular LDH. However, when MCT4 is reduced, more HP lactate molecules are near LDH and can be converted to pyruvate. Thus we show that bidirectional exchange is modulated by MCT4, a transporter often highly expressed in aggressive cancers [24,25].

Finally, feasibility of the application of the Ultrafast EXSY technique *in vivo* was tested in a single experiment comparing a normal kidney and a kidney in a mouse with implanted UOK262 cell line under the renal capsule (Fig. 5B). Comparing the RCC tumor model kidney to the contralateral normal kidney, we observed increased conversion of HP pyruvate-to-lactate and reduced conversion HP lactate-to-pyruvate, which based on our cell studies, suggests high LDH and high MCT4, respectively (Fig. 5D). However, more experiments are needed to prove this hypothesis. More significantly, this single proof-of-concept study shows that bidirectional exchange can be observed *in vivo* for pyruvate–lactate, pyruvate–alanine, and pyruvate–hydrate and that they can be resolved in time.

5. Conclusions

In this work, we present a new UltraFast method for acquiring dynamic 2D EXchange SpectroscopY (UF-EXSY) within a single acquisition using phase accrual. The presented dynamic UF-EXSY pulse sequence is rapid and does not require renewable longitudinal magnetization making it ideal for hyperpolarized substrates. This method overcomes the three main challenges associated with 2D NMR of hyperpolarized substrates: (1) 2D NMR experiments are time intensive, (2) longitudinal magnetization is not renewable, and (3) the signal decays quickly requiring fast acquisition.

Additionally, we show that 2D NMR of hyperpolarized substrates can provide a new tool to probe the directionality of exchange and flux of metabolic pathways. The technique provided insights on the effect of transporters on exchange as well as showed the potential of using bidirectional exchange as a marker of transport. Here we show that bidirectional exchange is modulated by MCT4 in metastatic RCC cell line.

Outside of the field of oncology, the potential applications of this technique are broad including applications such as solvent hydrogen-exchange, protein interactions, protein folding, and conformational changes such as cis-trans isomerizations and domain movements as wells as to investigate multistep chemical reactions. More broadly the utilization of phase in 2D NMR acquisitions could be adapted to quickly acquire sparse 2D spectra for other nuclei such as ^{1}H, ^{15}N, ^{31}P, and ^{129}Xe.

6. Uncited references

[6,16].

Supplementary Material

Refer to Web version on PubMed Central for supplementary material.

Acknowledgments

The authors acknowledge Dr. Kayvan Keshari and Mark Van Criekinge for their development of the bioreactor system as well as Dr. Michael Lustig and Peter Shin for discussions on optimization, Drs. John Pauly and Adam Kerr for discussions on stimulated echoes, and Dr. Christian Frezza for discussions of abnormal cancer metabolism in renal cell carcinomas. The DNP polarizers and related infrastructure were supported by an NIH center Grant (P41EB013598). This study was also supported by NIH Grants R00-EB012064 (to PEZL), R01-EB016741 (to PEZL) as well as a DOD CA110032 Visionary Post-doctoral Fellowship (to RS).

References

1. Frydman L, Blazina D. Ultrafast two-dimensional nuclear magnetic resonance spectroscopy of hyperpolarized solutions. Nat Phys. 2007; 3:415–419.
2. Ardenkjaer-Larsen JH, et al. Increase in signal-to-noise ratio of >10,000 times in liquid-state NMR. Proc Natl Acad Sci. 2003; 100:10158–10163. [PubMed: 12930897]
3. Mishkovsky M, Frydman L. Progress in hyperpolarized ultrafast 2D NMR spectroscopy. Chem Phys Chem. 2008; 9:2340–2348. [PubMed: 18850607]
4. Shapira B, Frydman L. Arrayed acquisition of 2D exchange NMR spectra within a single scan experiment. J Magn Reson. 2003; 165:320–324. [PubMed: 14643716]
5. Larson PEZ, Kerr AB, Swisher CL, Pauly JM, Vigneron DB. A rapid method for direct detection of metabolic conversion and magnetization exchange with application to hyperpolarized substrates. J Magn Reson. 2012; 225:71–80. [PubMed: 23143011]
6. Harris T, Eliyahu G, Frydman L, Degani H. Kinetics of hyperpolarized 13C1-pyruvate transport and metabolism in living human breast cancer cells. Proc Natl Acad Sci. 2009; 106:18131–18136. [PubMed: 19826085]
7. Day SE, et al. Detecting response of rat C6 glioma tumors to radiotherapy using hyperpolarized [1-^{13}C]pyruvate and ^{13}C magnetic resonance spectroscopic imaging. Magn Reson Med. 2011; 65:557–563. [PubMed: 21264939]
8. Keshari KR, et al. Hyperpolarized 13C-pyruvate magnetic resonance reveals rapid lactate export in metastatic renal cell carcinomas. Cancer Res. 2013; 73:529–538. [PubMed: 23204238]
9. Kurhanewicz J, et al. Analysis of cancer metabolism by imaging hyperpolarized nuclei: prospects for translation to clinical research. Neoplasia. 2011; 13:81–97. [PubMed: 21403835]
10. Nelson SJ. Metabolic imaging of patients with prostate cancer using hyperpolarized [1-13C]pyruvate. Sci Transl Med. 2013; 5:198ra108.
11. Park JM, et al. Metabolite kinetics in C6 rat glioma model using magnetic resonance spectroscopic imaging of hyperpolarized [1-^{13}C]pyruvate. Magn Reson Med. 2012; 68:1886–1893. [PubMed: 22334279]
12. Zierhut ML, et al. Kinetic modeling of hyperpolarized 13C1-pyruvate metabolism in normal rats and TRAMP mice. J Magn Reson. 2010; 202:85– 92. [PubMed: 19884027]
13. Swisher CL, et al. Quantitative measurement of cancer metabolism using stimulated echo hyperpolarized carbon-13 MRS. Magn Reson Med. 2014; 71:1–11. [PubMed: 23412881]
14. Mullen AR, et al. Reductive carboxylation supports growth in tumour cells with defective mitochondria. Nature. 2012; 481:385–388. [PubMed: 22101431]
15. Mullen AR, et al. Oxidation of alpha-ketoglutarate is required for reductive carboxylation in cancer cells with mitochondrial defects. Cell Rep. 2014; 7:679–690.

16. Menendez JA, Lupu R. Fatty acid synthase and the lipogenic phenotype in cancer pathogenesis. Nat Rev Cancer. 2007; 7:763–777. [PubMed: 17882277]
17. Hu S, et al. 13C-pyruvate imaging reveals alterations in glycolysis that precede c-Myc-induced tumor formation and regression. Cell Metab. 2011; 14:131– 142. [PubMed: 21723511]
18. Dang CV. MYC, microRNAs and glutamine addiction in cancers. Cell Cycle. 2009; 8:3243–3245. [PubMed: 19806017]
19. Son J, et al. Glutamine supports pancreatic cancer growth through a KRAS-regulated metabolic pathway. Nature. 2013; 496:101–105. [PubMed: 23535601]
20. Wise DR, Thompson CB. Glutamine addiction: a new therapeutic target in cancer. Trends Biochem Sci. 2010; 35:427–433. [PubMed: 20570523]
21. Reed GD, et al. High resolution (13)C MRI with hyperpolarized urea: in vivo T(2) mapping and (15)N labeling effects. IEEE Trans Med Imaging. 2014; 33:362–371. [PubMed: 24235273]
22. Wilson DM, et al. Multi-compound polarization by DNP allows simultaneous assessment of multiple enzymatic activities in vivo. J Magn Reson. 2010; 205:141–147. [PubMed: 20478721]
23. Dimmer KS, Friedrich B, Lang F, Deitmer JW, Broer S. The low-affinity monocarboxylate transporter MCT4 is adapted to the export of lactate in highly glycolytic cells. Biochem J. 2000; 350:219–227. [PubMed: 10926847]
24. Gotanda Y, et al. Expression of monocarboxylate transporter (MCT)-4 in colorectal cancer and its role: MCT4 contributes to the growth of colorectal cancer with vascular endothelial growth factor. Anticancer Res. 2013; 33:2941–2947. [PubMed: 23780984]
25. Lim KS, et al. Inhibition of monocarboxylate transporter-4 depletes stem-like glioblastoma cells and inhibits HIF transcriptional response in a lactate-independent manner. Oncogene. 2013; 33:4433–4441. [PubMed: 24077291]

Appendix A. Supplementary material

Supplementary data associated with this article can be found, in the online version, at http://dx.doi.org/10.1016/j.jmr.2015.05.011.

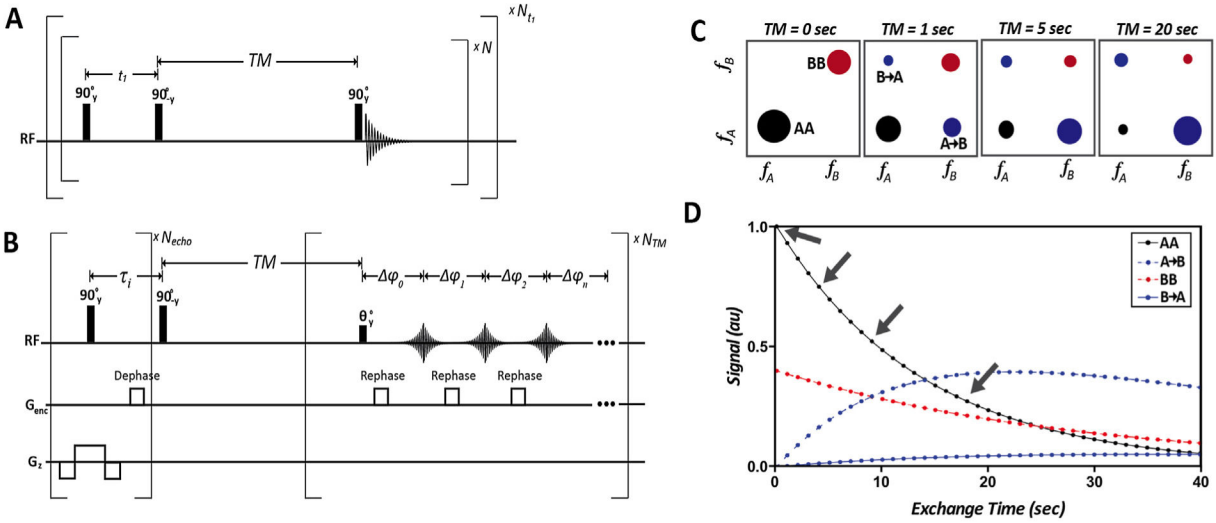

Fig. 1.

(A) Conventional Dynamic EXchange SpectroscopY (EXSY) requiring renewable longitudinal magnetization not available in hyperpolarized substrates and many repetitions to obtain the entire indirect spectral direction. (B) Dynamic UltraFast EXSY (UF-EXSY) pulse sequence is rapid and does not require renewable longitudinal magnetization making it ideal for hyperpolarized substrates. (C) Schematic of dynamic 2D exchange spectra and (D) simulated build up curves from four measured signal intensities in (c) which can be fit to an exchange model to extract kinetic rates of interconversion. Arrows denote time points shown in 2D spectra (c).

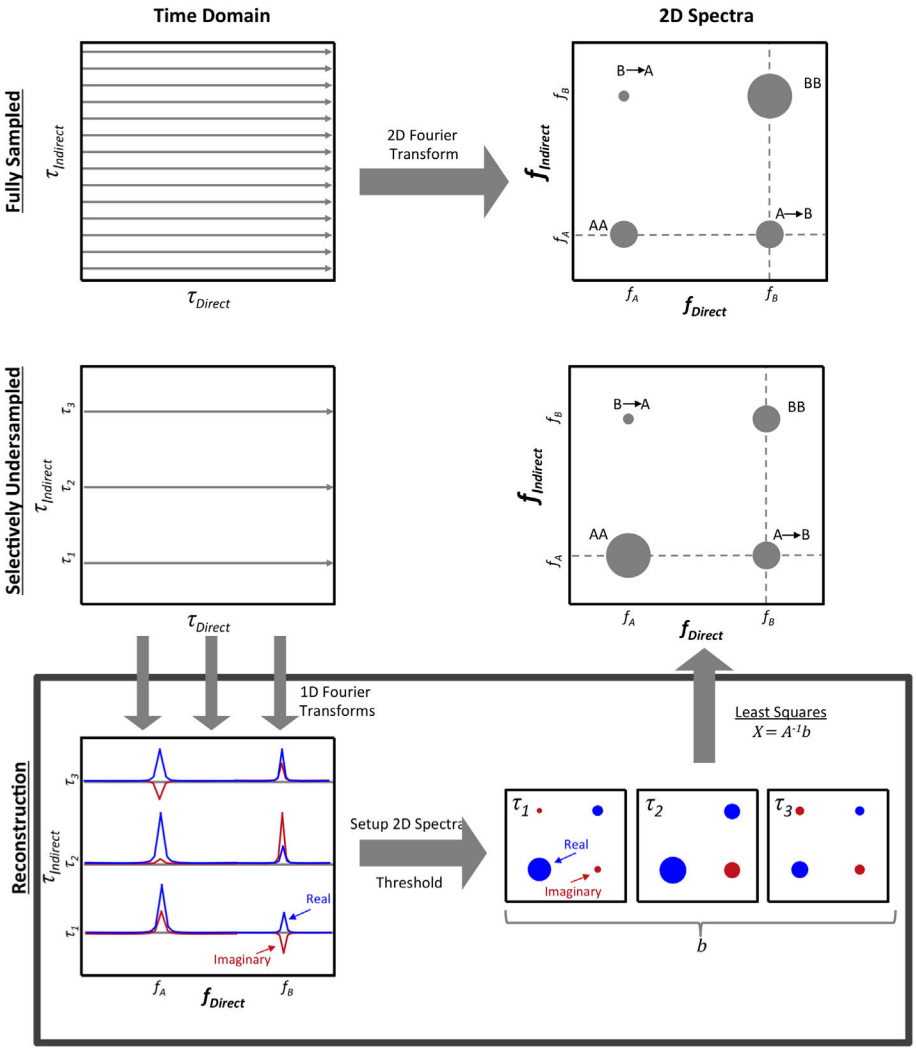

Fig. 2.

Schematic of Ultra FastEXchange SpectroscopY (UF-EXSY) reconstruction. Using conventional EXSY the 2D spectra can be reconstructed from the magnitude of the 1D spectrum but requires many τ repetitions. Using the UF-EXSY reconstruction the entire 2D spectra can be reconstructed from a few echoes with high spectral resolution in the indirect frequency direction equal to that of the direct frequency direction. For each frequency, *fi*, with a signal greater than the noise threshold in the direct frequency direction the cross peaks are calculated using Eq. (6) or with linear least squares based on the phase accrual and frequency difference between every other frequency with a signal also greater than the noise threshold. 2D spectra can be reconstructed from a single acquisition as long as he number of echoes is greater than the number of concomitant exchange pathways at a single resonance.

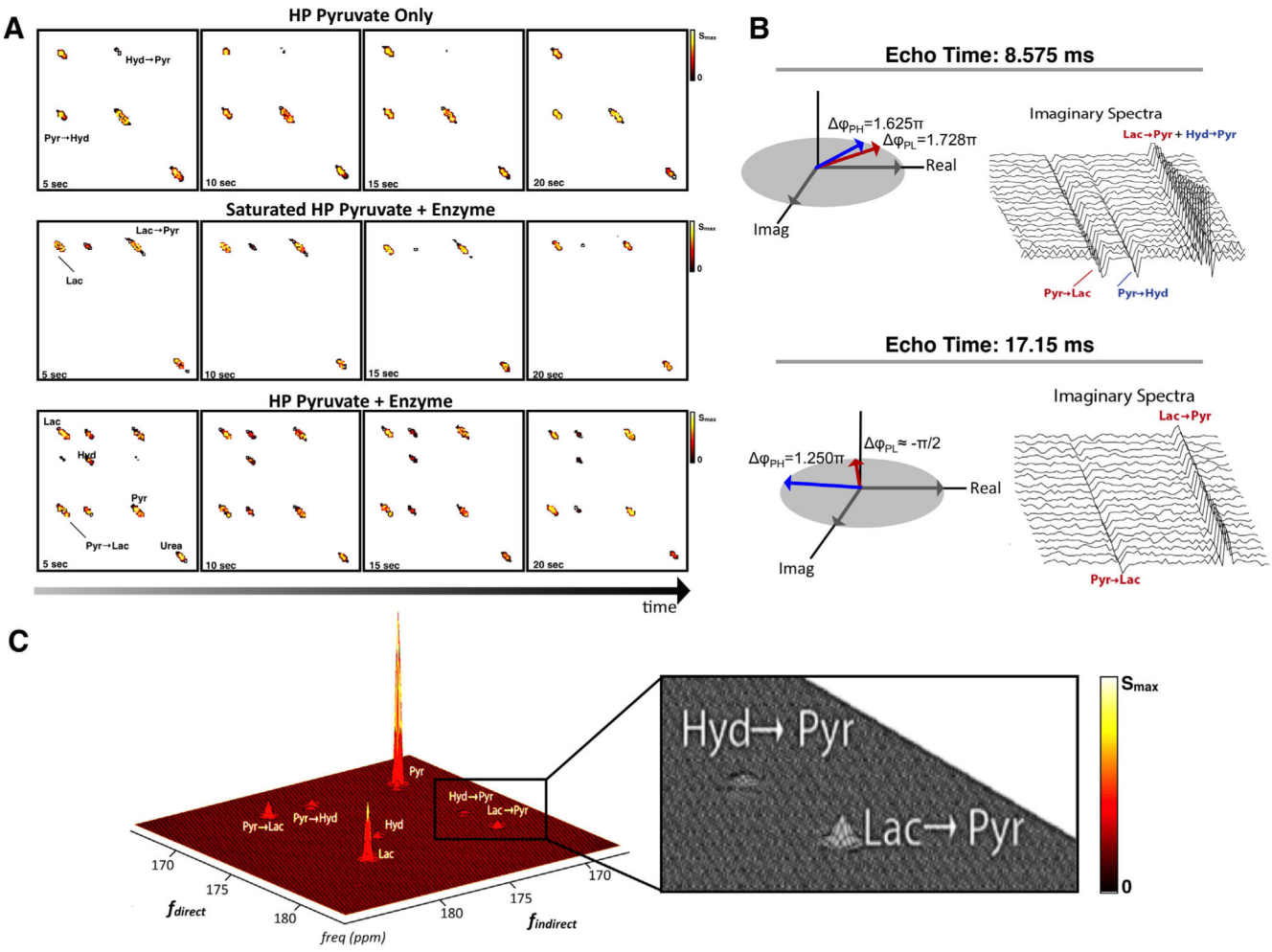

Fig. 3.

(A) Dynamic EXSY spectra of (top) pyruvate hydration co-polarized with ^{13}C-urea, (middle) pyruvate conversion to lactate via LDH enzyme and cofactor NADH with and (bottom) without saturation pulses on pyruvate. (B) Validation of phase encoding for multiple echoes. Schematic shows phase dependence of the (left) first and (right) second echo and their corresponding raw dynamic imaginary spectra from UOK262 renal cell carcinoma (RCC) cell-filled alginate microspheres (TR = 1 s) in MR-compatible bioreactor (C) and the 2D spectra (sum of all time points, TR = 1 s, *N* = 20) from the RCC cells.

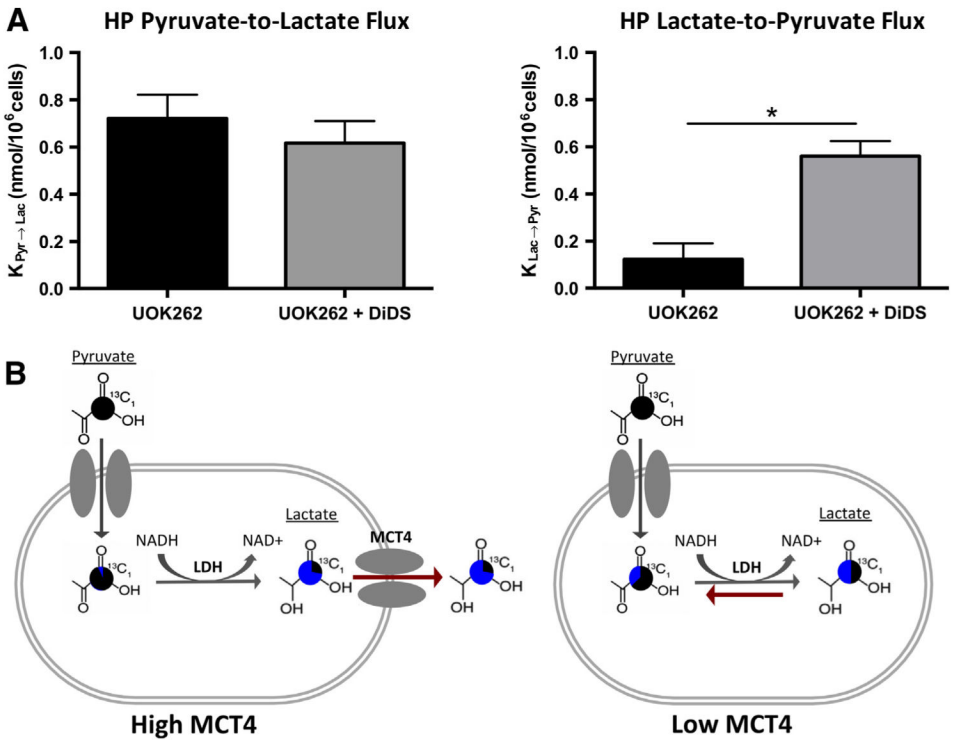

Fig. 4.

(A) Dynamic UltraFast 2D EXchange SpectroscopY (UF-EXSY) reveals high MCT4 in metastatic renal cell carcinomas and revels decreased conversion of lactate back to pyruvate with the efflux of lactate out of the cell. All values are reported as mean ± SE. *Denotes significant difference ($p < 0.05$). (B) Schematic of pyruvate and lactate exchange with high and low MCT4. Pie charts demonstrate the proportion of the label that is generated after encoding with “New” shown in blue and the proportion that were present during encoding, “Original” shown in black. (For interpretation of the references to color in this figure legend, the reader is referred to the web version of this article.)

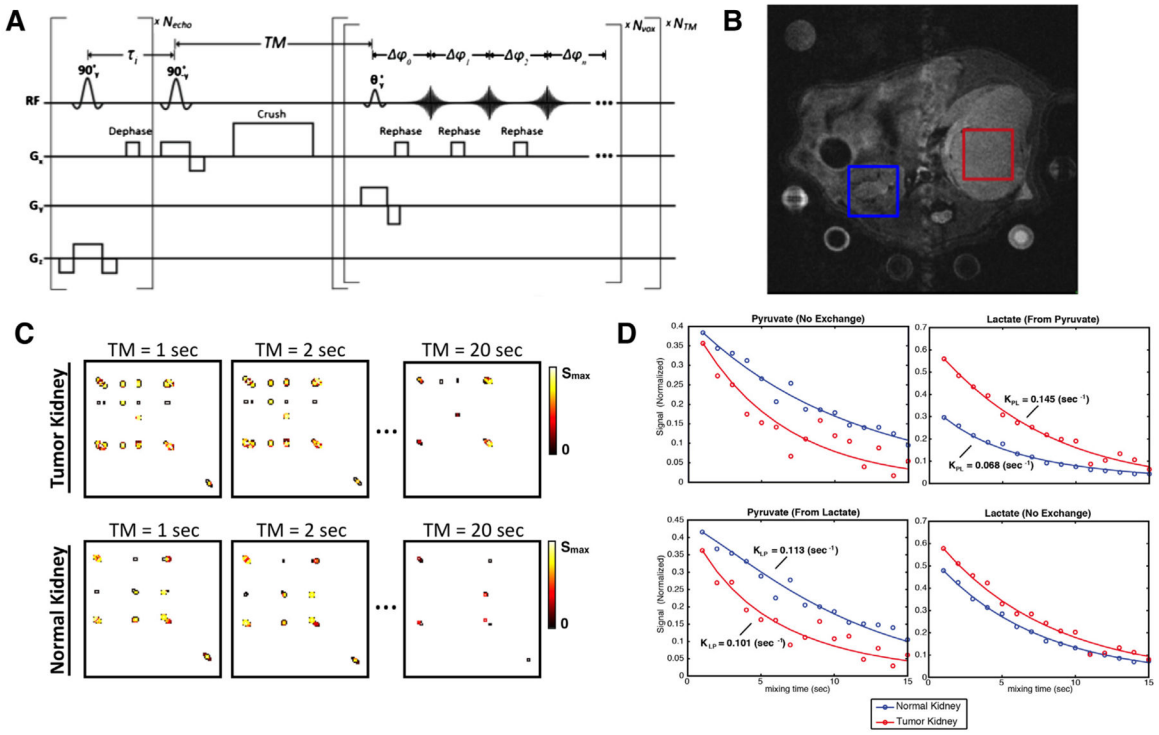

Fig. 5.

In vivo feasibility (A) Multivoxel pulse sequence for *in vivo* studies. (B) Location of voxels on T_2W anatomical image. One voxel was acquired in a UOK262 implanted tumor and the other was acquired in the contralateral normal kidney. Both voxels were acquired within a single acquisition. (C) Dynamic 2D spectra data and (D) Dynamic traces with corresponding fitted kinetic parameters show contrast between kidneys.